

On the trend of [Mg/Fe] among giant elliptical galaxies

Francesca Matteucci^{1,2}, Raffaella Ponzzone^{1,2}, and Brad K. Gibson³

¹ Dipartimento di Astronomia, Università di Trieste, Via G.B. Tiepolo, 11, I-34131 Trieste, Italy

² SISSA/ISAS, Via Beirut 2-4, I-34014 Trieste, Italy

³ Mt. Stromlo and Siding Spring Observatories, Australian National University, Weston Creek, ACT 2611, Australia

Received 17 February 1998 / Accepted 16 March 1998

Abstract. We revisit the problem of the flat slope of the Mg_2 versus $\langle Fe \rangle$ relationship found for nuclei of elliptical galaxies (Faber et al. 1992; Worthey et al. 1992; Carollo et al. 1993; Davies et al. 1993), indicating that the Mg/Fe ratio should increase with galactic luminosity and mass. We transform the abundance of Fe, as predicted by classic wind models and alternative models for the chemical evolution of elliptical galaxies, into the metallicity indices Mg_2 and $\langle Fe \rangle$, by means of the more recent index calibrations and show that none of the current models for the chemical evolution of elliptical galaxies is able to reproduce exactly the observed slope of the $\langle Fe \rangle$ versus Mg_2 relation, although the existing spread in the data makes this comparison quite difficult. In other words, we can not clearly discriminate between models predicting a decrease (classic wind model) or an increase of such a ratio with galactic mass. The reason for this resides in the fact that the available observations show a large spread due mostly to the errors in the derivation of the $\langle Fe \rangle$ index. In our opinion this fact prevents us from drawing any firm conclusion on the behaviour of Mg and Fe in these galaxies. Moreover, as already shown by other authors, one should be careful in deriving trends in the real abundances just from the metallicity indices, since these latter depend also on other physical parameters than the metallicity. This is an important point since abundance ratios have been proven to represent strong constraints for galaxy formation mechanisms.

Key words: nuclear reactions, nucleosynthesis, abundances – galaxies: elliptical and lenticular, cD – galaxies: evolution – galaxies: abundances

1. Introduction

Elliptical galaxies do not show the presence of HII regions and it is not possible to resolve single stars in them in order to measure photospheric abundances. Therefore, most of the information on these objects is obtained from their integrated properties:

abundances are derived either through colors or integrated spectra and in both cases the derived information is a complicated measure of metallicity and age (the well known age-metallicity degeneracy). The most common metallicity indicators are Mg_2 and $\langle Fe \rangle$, as originally defined in Faber et al. (1977; 1985). Population synthesis techniques are adopted to analyze the integrated properties of ellipticals and to derive an estimate of their real abundances. Unfortunately, they contain several uncertainties residing either in incomplete knowledge of stellar evolution or in deficiencies in stellar libraries, as discussed in Charlot et al. (1996). In recent years more and more population synthesis models (Bruzual and Charlot, 1993; Buzzoni et al., 1992; Bressan et al., 1994; Gibson, 1997; Bressan et al., 1996; Gibson and Matteucci, 1997; Tantalo et al., 1998) have appeared but the basic uncertainties still remain. In this paper we want to focus our attention about the comparison between theoretical model results and metallicity indicators. In this framework we will analyze the relationship between $\langle Fe \rangle$ and Mg_2 and its implications for the mechanism of galaxy formation.

Several authors (Faber et al. 1992; Worthey et al. 1992; Carollo et al. 1993; Davies et al. 1993; Carollo and Danziger 1994a,b), from comparison of the observed indices with synthetic indices, concluded that the average $[\langle Mg/Fe \rangle]_*$ in giant ellipticals must be larger than the solar value. This result was also confirmed by the analysis of Weiss et al. (1995) who made use, for the first time, of stellar evolutionary tracks calculated under the assumption of non-solar ratios. The same authors found that the $\langle Fe \rangle$ versus Mg_2 relation among nuclei of giant ellipticals is rather flat and flatter than within galaxies. From the flat behavior of $\langle Fe \rangle$ vs. Mg_2 the same authors inferred that the abundance of Mg should increase faster than the abundance of Fe among nuclei of giant ellipticals. This conclusion is at variance with the predictions of supernova-driven wind models of ellipticals (Arimoto and Yoshii, 1987; Matteucci and Tornambè 1987). In fact, Matteucci and Tornambè (1987) showed that, in the framework of the classic wind model for ellipticals, the [Mg/Fe] ratio is a decreasing function of the galactic mass and luminosity. The reason for this behavior is clear: if Fe is mostly produced by the supernovae of type Ia, as it seems to be the case in our Galaxy (Greggio and Renzini 1983; Matteucci and Greggio 1986), whereas Mg is mostly originating from supernovae of type II, then the iron production is delayed relative

Send offprint requests to: F. Matteucci

to that of Mg and its abundance should be larger in more massive galaxies which develop a wind later than the less massive ones. All of this is valid under the assumption that after the onset of a galactic wind star formation should stop or should be negligible, which is a reasonable assumption for elliptical galaxies. Faber et al. (1992) proposed alternative scenarios to the classic supernova driven wind model, as originally proposed by Larson (1974). They suggested three different scenarios all based on the assumption that Mg is produced by type II supernovae and Fe is mostly produced by type Ia supernovae: i) a selective loss of metals, ii) a variable initial mass function (IMF) and iii) different timescales for star formation. These hypotheses were discussed by Matteucci (1994), who tested them in the context of chemical evolution models. In the hypothesis of the different timescales for star formation Matteucci (1994) suggested that the more massive ellipticals might experience a much stronger and faster star formation than less massive ellipticals leading to a situation where the most massive objects are able to develop galactic winds before the less massive ones. She called this case “inverse wind model”. On the other hand, in the classic wind model of Larson (1974) the efficiency of star formation was the same for all galaxies thus leading to the fact that the galactic wind in more massive systems occurs later than in less massive ones, due to their deeper potential well. In the models of Arimoto and Yoshii (1987) and Matteucci and Tornambè (1987) the efficiency of star formation was a decreasing function of galactic mass, based on the assumption that the timescale for star formation is proportional to the cloud-cloud collision timescale which, in turn, is proportional to the gas density. Therefore, since in this monolithic collapse picture the gas density decreases with the galactic mass, the galactic wind was even more delayed for the most massive systems. Matteucci (1994) proposed, as an alternative, a star formation efficiency increasing with the galactic mass and she justified this assumption by imagining that giant elliptical galaxies, instead of forming through a monolithic collapse of a gas cloud, form by merging of gaseous protoclouds. The merging process can, in fact, produce higher densities for increasing galactic mass and/or higher cloud-cloud collision velocities resulting in a faster star formation process. In such a model the galactic wind occurs earlier in massive than in smaller ellipticals thus producing the expected trend of an increasing [Mg/Fe] as a function of galactic mass. Matteucci (1994) also showed that a variable IMF with the slope decreasing with increasing galactic mass and luminosity can produce the same effect without an inverse wind situation. The reason for that resides in the fact that a flatter IMF slope favors massive stars relative to low and intermediate masses, thus favoring Mg production over Fe production. However, Matteucci (1994) could not translate the predicted abundances into Mg_2 and $\langle Fe \rangle$ since there were no available calibrations for [Fe/H] versus $\langle Fe \rangle$ but only calibrations for $[Fe/H]$ vs. Mg_2 . Therefore she did not compare the predicted abundances with observations.

Recently, calibrations for the iron index have become available (Borges et al., 1995; Tantalò et al., 1998) and therefore in this paper we revisit the whole problem of inferring trends on the real abundances by metallicity indices and we discuss the

influence of the calibration relationships, which allow us to pass from indices to abundances, and we show that the inferred trend of Mg/Fe with galactic mass is not so clear when interpreted in terms of real abundances, thus warning us from drawing any firm conclusion on galaxy formation processes just on the basis of the observed behavior of $\langle Fe \rangle$ versus Mg_2 indices. The reason for that resides partly in the large spread present in the observational data and partly in the fact that metallicity indices depend not only on the abundances of single elements but also on the ages and on the metallicity distribution (Tantalò et al. 1998) of the different stellar populations present in elliptical galaxies.

In Sect. 2 we will discuss the chemical evolution model, in Sect. 3 we will define the average abundances of a composite stellar population, in Sect. 4 we will describe the model results and transform the predicted abundances into indices by means of the most recent metallicity calibrations. Finally in Sect. 5 some conclusions will be drawn.

2. The chemical evolution model

2.1. Basic equations

The adopted model of galactic evolution is that outlined by Matteucci and Gibson (1995) (hereafter MG95), where extensive descriptions and references can be found. The evolution of the abundances of several chemical species (H, He, C, N, O, Ne, Mg, Si and Fe) in the gas is followed, taking into account detailed nucleosynthesis from stars of all masses and SNe of types Ia, Ib, and II. We assume that ellipticals can be considered initially as homogeneous spheres of gas with luminous mass in the range $10^9 \rightarrow 1 \times 10^{12} M_\odot$. A single zone interstellar medium (ISM) with instantaneous mixing of gas is assumed throughout. The adopted age for all galaxy models is $t_G = 15$ Gyr.

The fundamental equations can be written as:

$$\begin{aligned} \frac{dG_i(t)}{dt} = & -\psi(t)X_i(t) + \int_{M_L}^{M_{BM}} \psi(t - \tau_m)Q_{mi}(t - \tau_m)\phi(m)dm \\ & + A \int_{M_{BM}}^{M_{BM}} \phi(m) \left[\int_{\mu_{min}}^{0.5} f(\mu)\psi(t - \tau_{m2})Q_{mi}(t - \tau_{m2})d\mu \right] dm \\ & + (1 - A) \int_{M_{BM}}^{M_{BM}} \psi(t - \tau_m)Q_{mi}(t - \tau_m)\phi(m)dm \\ & + \int_{M_{BM}}^{M_U} \psi(t - \tau_m)Q_{mi}(t - \tau_m)\phi(m)dm, \end{aligned} \quad (1)$$

where $G_i(t) = \rho_{gas}(t)X_i(t)/\rho(0)$ is the volume gas density in the form of an element i normalized to the initial total volume gas density. The quantity $X_i(t)$ represents the abundance by mass of an element i and by definition the summation over all the elements present in the gas mixture is equal to unity.

The various integrals in Eq. (1) represent the rates at which SNe (I and II) as well as single low and intermediate mass stars and single massive stars restore their processed and unprocessed material into the ISM (for a detailed description of the integrals see MG95; Matteucci and Greggio 1986). We only remind here that the quantity Q_{mi} represents the fraction of a star of mass

m which is restored into the ISM in the form of an element i and therefore contains the nucleosynthesis prescriptions that we assume to be the same as in MG95.

The star formation rate $\psi(t)$ is given by:

$$\psi(t) = \nu \rho_{\text{gas}}(t) / \rho(0). \quad (2)$$

i.e. normalized to the initial total volume density. $\psi(t)$ is assumed to drop to zero at the onset of the galactic wind. The quantity ν is expressed in units of Gyr^{-1} and represents the efficiency of star formation, namely the inverse of the time scale of star formation. The values adopted here for ν are the same as in Matteucci (1992) and Arimoto and Yoshii (1987). In one case we have adopted the prescription for the **inverse wind model** of Matteucci (1994). The difference between the two cases is that in Matteucci (1994) the **classic wind model** assumes that the efficiency of star formation decreases with increasing total galactic mass, as in Arimoto and Yoshii (1987), whereas in the inverse wind model the efficiency of star formation increases as the total galactic mass increases (similar in spirit to the SFR efficiency parametrization of Tinsley and Larson 1979) leading to a situation in which more massive galaxies experience a galactic wind before the less massive ones.

The quantity τ_m represents the lifetime of a star of mass m , and is taken from Padovani and Matteucci (1993).

2.2. Galactic winds

For gas to be expelled from a galaxy the following condition should be satisfied: the thermal energy of the gas heated by SN explosions should exceed the binding energy of the gas (Larson 1974). At this point the gas present in the galaxy is swept away and the subsequent evolution is determined only by the amount of matter and energy which is restored in to the ISM by the dying stellar generations. In particular, only low mass stars contribute to this evolutionary phase and, among the SNe, only SNe of type Ia (i.e. those SNe events whose progenitors have the longest lifetimes).

Therefore, in order to evaluate the time for the onset of a galactic wind we need to know the energy input from SNe and the binding energy of the gas as a function of time. The total thermal energy of the gas at time t , E_{thSN} , and the binding energy of the gas in presence of a diffuse halo of dark matter are calculated as described in Matteucci (1992). In particular, $E_{\text{thSN}}(t)$ is calculated by assuming that $\sim 70\%$ of the initial blast wave energy is transferred into the ISM as thermal energy by a SN remnant, if the time elapsed from the SN explosion is shorter than a SN remnant cooling time (Cox 1972). The percentage of transferred energy then decreases as a power law in time $\propto t^{-0.62}$ for times larger than the cooling time.

This is the same formulation used by Arimoto and Yoshii (1987), Matteucci and Tornambè (1987) and MG95 with the exception that we consider a more realistic cooling time (expressed in years) which takes into account that the gas density is changing with time and that part of the interstellar gas is in

Table 1. Model I-classic wind, $x=1.35$

$M_{\text{lum}}(M_{\odot})$	$\nu (\text{Gyr}^{-1})$	$R_{\text{eff}} (\text{kpc})$	$t_{\text{GW}} (\text{Gyr})$	$M_{\text{fin}} (M_{\odot})$
10^9	19.0	0.5	0.131	$0.658 \cdot 10^9$
10^{10}	14.6	1.0	0.286	$0.791 \cdot 10^{10}$
10^{11}	11.2	3.0	0.514	$0.974 \cdot 10^{11}$
10^{12}	8.6	10.0	0.955	$0.885 \cdot 10^{12}$

Table 2. Model II- classic wind, $x=0.95$

$M_{\text{lum}}(M_{\odot})$	$\nu (\text{Gyr}^{-1})$	$R_{\text{eff}} (\text{kpc})$	$t_{\text{GW}} (\text{Gyr})$	$M_{\text{fin}} (M_{\odot})$
10^9	19.0	0.5	0.069	$0.246 \cdot 10^9$
10^{10}	14.6	1.0	0.117	$0.388 \cdot 10^{10}$
10^{11}	11.2	3.0	0.403	$0.668 \cdot 10^{11}$
10^{12}	8.6	10.0	0.660	$0.913 \cdot 10^{12}$

Table 3. Model III- inverse wind, $x=0.95$

$M_{\text{lum}}(M_{\odot})$	$\nu (\text{Gyr}^{-1})$	$R_{\text{eff}} (\text{kpc})$	$t_{\text{GW}} (\text{Gyr})$	$M_{\text{fin}} (M_{\odot})$
10^9	2.	0.5	1.200	$0.502 \cdot 10^9$
10^{10}	5.	1.0	0.897	$0.605 \cdot 10^{10}$
10^{11}	11.	3.0	0.408	$0.665 \cdot 10^{11}$
10^{12}	20.	10.0	0.205	$0.841 \cdot 10^{12}$

the form of He:

$$t_c = 5.7 \cdot 10^4 [2.99 \cdot 10^{-3} (M_{\text{gas}}(t)/10^{12} M_{\odot}) \cdot (M_{\text{lum}}/10^{12} M_{\odot})^{-1.65}]^{-0.53} \text{ years}. \quad (3)$$

Other formulations of the energy input from SNe can be found in Gibson (1997) and Gibson and Matteucci (1997).

The energetic input from stellar winds in massive stars is ignored, since for normal ellipticals it is negligible compared to the SN thermal energy contribution, as shown by Gibson (1994).

The galactic wind may last only for few 10^8 years or continue until the present time depending crucially on the assumptions about the thermal energy of the gas and the potential energy of the gas. Unfortunately, none of these quantities is well known. The time for the occurrence of the galactic wind, t_{GW} , either increases with the galactic mass as a consequence of the potential well increasing with galactic mass together with the efficiency of star formation decreasing with galactic mass (classic wind model), or decreases with the galactic mass if the efficiency of star formation is strongly increasing with galactic mass (inverse wind model), as can be seen in Table 3, and will be discussed in Sect. 4.

3. The average metallicity of a composite stellar population

In order to compare model results with observations we should first calculate the average abundances of Mg and Fe of the

Table 4. Model IV-classic wind, variable IMF

$M_{lum}(M_{\odot})$	$\nu (Gyr^{-1})$	R_{eff} (kpc)	t_{GW} (Gyr)	$M_{fin} (M_{\odot})$	IMF slope
10^9	19.0	0.5	0.163	$0.936 \cdot 10^9$	2.0
10^{10}	14.6	1.0	0.237	$0.945 \cdot 10^{10}$	1.7
10^{11}	11.2	3.0	0.514	$0.974 \cdot 10^{11}$	1.35
10^{12}	8.6	10.0	0.660	$0.912 \cdot 10^{12}$	0.95

Table 5. Model V- classic wind, time variable IMF

$M_{lum}(M_{\odot})$	$\nu (Gyr^{-1})$	R_{eff} (kpc)	t_{GW} (Gyr)	$M_{fin} (M_{\odot})$
10^9	19.0	0.5	0.073	$0.276 \cdot 10^9$
10^{10}	14.6	1.0	0.223	$0.764 \cdot 10^{10}$
10^{11}	11.2	3.0	0.601	$0.960 \cdot 10^{11}$
10^{12}	8.6	10.0	2.205	$0.995 \cdot 10^{12}$

Table 6. Model VI- inverse wind, $x=0.8$

$M_{lum}(M_{\odot})$	$\nu (Gyr^{-1})$	R_{eff} (kpc)	t_{GW} (Gyr)	$M_{fin} (M_{\odot})$
10^9	4.0	0.5	0.220	$0.320 \cdot 10^9$
10^{10}	18.0	1.0	0.110	$0.430 \cdot 10^{10}$
10^{11}	32.0	3.0	0.090	$0.550 \cdot 10^{11}$
10^{12}	75.0	10.0	0.030	$0.450 \cdot 10^{12}$

composite stellar population of the given galaxies. The average metallicity or abundance in general which should be compared with the indices should be averaged on the visual light, namely:

$$\langle X_i \rangle_L = \frac{\sum_{ij} n_{ij} X_i L_{V_j}}{\sum_{ij} n_{ij} L_{V_j}} \quad (4)$$

where n_{ij} is the number of stars in the abundance interval X_i and luminosity L_{V_j} . On the other hand, the real average abundance should be the mass-averaged one, namely:

$$\langle X_i \rangle_M = \frac{1}{S_1} \int_0^{S_1} X_i(S) dS \quad (5)$$

where the subscript 1 refers to the specific time t_1 (the present time) and S_1 is the total mass of stars ever born. Here we will use Eq. (5) in order to compare model results with indices and the reason is that we want to compare our results with previous ones (Matteucci 1994; MG95), and because for giant ellipticals the difference between the mass-averaged metallicity and the luminosity-averaged one is negligible (Yoshii and Arimoto, 1987; Gibson 1997). On the other hand, in smaller systems the difference between the two abundances is not negligible due to the contribution to the light of low metallicity red giants (Greggio 1996). We will show in Sect. 4 that in the cases studied here $\langle X_i \rangle_L \simeq \langle X_i \rangle_M$.

4. Model results

In this section we will show the results of several models and we will convert, by means of the available calibrations, the average stellar abundances of Mg and Fe, $[\langle Mg/H \rangle]_*$ and $[\langle Fe/H \rangle]_*$, as predicted for elliptical galaxies of different mass, into the metallicity indices Mg_2 and $\langle Fe \rangle$, respectively.

Let us discuss first the metallicity calibrations. Relations linking the strength of metallicity indices to real abundances can be either empirical or theoretical. In the past few years several attempts have been made to calibrate the strength of Mg_2 against [Fe/H] which has always been considered as the measure of the “metallicity” in stars. It should be said that this is not entirely correct since we know that Mg does not evolve in lockstep with iron in the solar neighborhood nor in elliptical galaxies, due to the different timescales of production of these two elements. It would be much better to calibrate Mg_2 versus [Mg/H] in order to avoid confusion. Calibrations of Mg_2 versus $\langle Fe \rangle$ are from Mould (1978), Burstein (1979), Peletier (1989), Buzzoni et al. (1992), Worthey et al. (1992). In all of these calibrations the ratio [Mg/Fe] is assumed to be solar, at variance with the indication arising from population synthesis models showing an overabundance of Mg relative to iron in the nuclei of giant ellipticals (Faber et al. 1992; Worthey et al. 1992; Davies et al. 1993; Weiss et al. 1995).

More recently, Barbuy (1994), Borges et al. (1995) and Tantalo et al. (1998) took into account non-solar ratios of [Mg/Fe] in their calibrations. In addition, some of them (Borges et al. 1995; Tantalo et al. 1998) produced synthetic $\langle Fe \rangle$ indices thus allowing us to calibrate [Fe/H] also against $\langle Fe \rangle$. This allows us to transform [Fe/H] in to Mg_2 and $\langle Fe \rangle$, although many uncertainties are involved in this exercise, mainly because, in this way, the derivations of Mg_2 and $\langle Fe \rangle$ are not independent.

We run several models, in particular: Model I, which is the classic wind model, as described in MG95, with a Salpeter (1955) IMF (namely an IMF with power index $x=1.35$ over a mass range $0.1 \leq M/M_{\odot} \leq 100$); Model II, which is the classic wind model with the Arimoto and Yoshii (1987) IMF (namely an IMF with power index $x=0.95$ over the same mass range of the Salpeter one); Model III, which is the equivalent of the inverse wind model, as described in Matteucci (1994) with the Arimoto and Yoshii (1987) IMF; Model IV which is the equivalent of the model with variable IMF, as described in Matteucci (1994), which assumes that ellipticals of smaller mass

have a steeper IMF than the more massive ones. It is worth noting that the slope of the IMF is kept constant inside a galaxy. In particular, we vary the slope of the IMF from the Salpeter one to the Arimoto and Yoshii one passing from a galaxy with initial luminous mass of $10^{11}M_{\odot}$ to a galaxy with $10^{12}M_{\odot}$. This particular assumption can reproduce the observed tilt of the fundamental plane seen edge-on, namely the increase of M/L versus L as observed by Bender et al. (1992).

Model V assumes a time-variable IMF as suggested by Padoan et al. (1997) and will be discussed in a forthcoming paper. In this formulation the IMF slope varies as a function of gas density and gas velocity dispersion, favoring the formation of massive stars at early epochs.

Model VI assumes a constant IMF with a slope $x=0.8$ and a star formation efficiency which varies more strongly with the luminous mass than in Model III. The slope $x=0.8$ is the limiting slope that we can accept to obtain a realistic M/L_B ratio for ellipticals, as discussed in Padovani and Matteucci (1993).

The model parameters are described in Tables 1-6 where we list the luminous masses in column 1, the star formation efficiency (in units of Gyr^{-1}) in column 2, the effective radius (in units of Kpc) in column 3, the time for the occurrence of the galactic wind (in Gyr) in column 4 and the final galactic luminous mass in column 5. For model IV is shown also the slope of the IMF in column 6.

We then calculate the average $[\langle Fe/H \rangle]_*$ and $[\langle Mg/Fe \rangle]_*$ for the stellar component of ellipticals by using Eq. (6) and finally we transform these abundances to observed Mg_2 and $\langle Fe \rangle$ line indices. In Tables 7-12 we show the results for different models and for the calibration of Tantaló et al. (1998). In particular, in Tables 7-12 we show the luminous mass in column 1, the $[\langle Fe/H \rangle]_*$ in the second column, the $[\langle Mg/Fe \rangle]_*$ in column 3 and in column 4 and 5 the Mg_2 and the $\langle Fe \rangle$ indices, respectively. As already said, only the calibrations of Tantaló et al. (1998) and Borges et al. (1995) allow us to transform $[Fe/H]$ into $\langle Fe \rangle$ and therefore to compare model results with the data showing the behavior of Mg_2 vs. $\langle Fe \rangle$ among nuclei of giant ellipticals. In particular, starting from the synthetic indices of Tantaló et al. (1998) calculated for a fixed [Mg/Fe] and a fixed [Fe/H] we derived calibration relationships of the type:

$$Mg_2 = f([Fe/H], [Mg/Fe]) \quad (6)$$

$$\langle Fe \rangle = g([Fe/H], [Mg/Fe]) \quad (7)$$

which allowed us to derive the indices for any [Fe/H] and [Mg/Fe]. The calibrations we have adopted are:

$$Mg_2 = 0.233 + 0.217[Mg/Fe] + (0.153 + 0.120[Mg/Fe]) \cdot [Fe/H] \quad (8)$$

$$\langle Fe \rangle = 3.078 + 0.341[Mg/Fe] + (1.654 - 0.307[Mg/Fe]) \cdot [Fe/H] \quad (9)$$

In Fig. 1 we show the metallicity indices obtained by means of the already mentioned calibrations compared with the data (Gonzalez 1993; Worthey et al. 1992; Carollo and Danziger 1994a,b). As one can easily see the data present a large spread, mostly due to the uncertainties in deriving the $\langle Fe \rangle$ indices. In particular, in Fig 1a we show the observed and predicted behavior of $\langle Fe \rangle$ vs. Mg_2 when Model I is adopted. The bestfit to the data implies the following relation, $\langle Fe \rangle = 3.94Mg_2 + 1.83$, and is indicated in the figure. However, the spread in the data is large and this prevents us from drawing strong conclusions about a possible trend. The dotted lines in Fig. 1a represent the predictions of Model I obtained by means of the calibrations described before and adopting the same [Mg/Fe] ratio as predicted by the models, as one can see in Table 7. The agreement with the observed trend is not so good, showing that the slope of the predicted relation is steeper than that shown by the data and that the predicted Mg_2 values do not cover the entire range in Mg_2 . This is mostly due to the assumed IMF since Model II, which assumes a flatter IMF, predicts values for Mg_2 which cover the whole range (see Fig. 2a).

In Fig. 1b we show the predicted and observed mass-metallicity (Mg_2) relationship. The data are from Carollo et al. (1993). The best-fit to these data indicate $Mg_2 = 0.02 \log M_{tot} + 0.08$, where M_{tot} is the total galactic mass (dark+luminous). The classic wind model recovers the slope of the Mg_2 – mass relation, but with a zeropoint offset of $\Delta Mg_2 \simeq 0.05$ with respect to the observed distribution.

On the other hand, the classic wind model with the Arimoto and Yoshii (1987) IMF (Model II), as shown in Fig. 2b, predicts a slope much steeper than the observed one, although it agrees better than Model I with the $\langle Fe \rangle$ vs. Mg_2 relation shown in Fig. 2a. It is worth noting that the Arimoto and Yoshii (1987) IMF well reproduces the abundances in the intergalactic medium (MG95; Gibson 1997; Gibson and Matteucci 1997). It is worth noting that in Figs. 1a and 2a and in all the others we show also the relation between real abundances predicted by our models. The relation between $[\langle Fe/H \rangle]_*$ and $[\langle Mg/H \rangle]_*$, arbitrarily translated in the plot of $\langle Fe \rangle$ versus Mg_2 , is indicated by the dashed lines. This is done only with the purpose of comparing the slope of the relation between real abundances with that of the relation between indices and they are very similar, indicating that the adopted calibration does not modify the predicted relation between Mg and Fe abundances. One of the main reasons for that is the adopted calibration which accounts for the right $[\langle Mg/Fe \rangle]_*$ ratio for each galaxy.

In Fig. 3a,b we show the predictions of the inverse wind model of Matteucci (1994) which predicts a stellar $[\langle Mg/Fe \rangle]_*$ increasing with galactic mass. The slope of the $\langle Fe \rangle$ versus Mg_2 relation is in better agreement than in the previous models, and the slope of the Mg_2 vs. mass relation is also acceptable although the absolute values of the indices are too high.

In Fig. 4a,b we show the results of Model IV with a variable IMF from galaxy to galaxy, which also predicts increasing $[\langle Mg/Fe \rangle]_*$ ratios with galactic mass. The agreement with the $\langle Fe \rangle$ vs. Mg_2 data is marginally acceptable, but the slope

Table 7. Model I- classic wind, $x=1.35$

$\log M_{lum}(M_{\odot})$	$[< Fe/H >]_*$ (dex)	$[< Mg/Fe >]_*$ (dex)	Mg_2 (mag)	$< Fe >$ (\AA)
9.	-0.395	0.262	0.217	2.545
10.	-0.190	0.224	0.247	2.853
11.	-0.095	0.187	0.257	2.990
12.	-0.007	0.130	0.260	3.112

Table 8. Model II- classic wind, $x=0.95$

$\log M_{lum}(M_{\odot})$	$[< Fe/H >]_*$ (dex)	$[< Mg/Fe >]_*$ (dex)	Mg_2 (mag)	$< Fe >$ (\AA)
9.	-0.833	0.397	0.152	1.937
10.	-0.034	0.329	0.298	3.137
11.	0.388	0.288	0.368	3.783
12.	0.502	0.264	0.383	3.957

Table 9. Model III- inverse wind, $x=0.95$

$\log M_{lum}(M_{\odot})$	$[< Fe/H >]_*$ (dex)	$[< Mg/Fe >]_*$ (dex)	Mg_2 (mag)	$< Fe >$ (\AA)
9.	0.197	0.262	0.326	3.477
10.	0.334	0.274	0.355	3.700
11.	0.384	0.290	0.368	3.777
12.	0.317	0.308	0.360	3.678

of the mass-metallicity relation is too steep and the predicted absolute values of Mg_2 are too low. The low absolute values of Mg_2 are due to the fact that we used slopes steeper than the Salpeter (1955) one for the less massive galaxies and such slopes are not suitable for elliptical galaxies (see MG95) since they predict too low metallicities. However, other numerical experiments, where we used a variable IMF but with flatter slopes for each galactic mass (from $x=1.4$ in low mass galaxies to $x=0.8$ in high mass galaxies), have shown that there is a negligible difference in the predicted $< Fe >$ vs. Mg_2 relation while the mass-metallicity relation gets worse.

In Fig. 5a,b we show the predictions of Model V calculated with the time-variable IMF as suggested by Padoan et al. (1997) and adapted to elliptical galaxies. The slope of this IMF is decreasing with time thus favoring massive stars at early epochs. A similar although more complex formulation of the Padoan et al. (1997) IMF has been recently adopted by Chiosi et al. (1998). The model behaves like a classic wind model, in the sense that the galactic wind occurs first in small galaxies and later in the more massive ones. Concerning the predicted indices, Fig. 5a shows that the Mg_2 decreases for massive objects, due to the fact that the IMF in these galaxies is less biased towards massive stars than in smaller systems. This is, in turn, due to the fact that the slope of the IMF is inversely proportional to the gas density which is lower in more massive objects. This model predicts a

sort of bimodal behavior for the Mg_2 vs. mass relation and it does not fit the data better than the other models.

Finally, in Fig. 6a,b the predictions of Model VI are shown. At variance with all the previous models, Model VI seems to reproduce well the observed slope of the $< Fe >$ vs. Mg_2 relation as well as the Mg_2 - mass relation. The main problem with this model is the fact that the predicted ranges of Mg_2 and $< Fe >$ are too narrow compared to the observations, especially the range of $< Fe >$. Another potential problem of this model is the predicted M/L_B ratio which is ~ 30 for each galaxy mass. This is a high value for ellipticals unless one believes in a Hubble constant $H_0 = 100 \text{Kms}^{-1} \text{Mpc}^{-1}$, as discussed in Padovani and Matteucci (1993).

In Figs. 7 and 8 we show the plot of the mass-metallicity (Mg_2) relation as predicted by Model I and Model II, obtained under different assumptions about the calibrating formula. As one can see, some of the calibrations give similar results such as those of Worthey et al. (1992), Casuso et al. (1996) and Buzzoni et al. (1992). These calibrations have in common the use of a solar ratio for [Mg/Fe] ([Mg/Fe]=0). On the other hand, the values of the indices obtained by using the calibrations of Barbuy (1994) and Tantalo et al. (1998) which adopt non-solar ratios, differ from the others and between themselves. It is worth noting that the use of different calibrations may lead even to different slopes for the Mg_2 - $\log M$ relationship.

Table 10. Model IV- classic wind, variable IMF

$\log M_{lum}(M_{\odot})$	$\langle [Fe/H] \rangle_*$ (dex)	$\langle [Mg/Fe] \rangle_*$ (dex)	Mg_2 (mag)	$\langle Fe \rangle$ (\AA)
9.	-1.450	0.149	0.002	0.800
10.	-0.834	0.169	0.125	1.800
11.	-0.095	0.187	0.257	2.990
12.	0.502	0.264	0.368	3.957

Table 11. Model V- classic wind, time variable IMF

$\log M_{lum}(M_{\odot})$	$\langle [Fe/H] \rangle_*$ (dex)	$\langle [Mg/Fe] \rangle_*$ (dex)	Mg_2 (mag)	$\langle Fe \rangle$ (\AA)
9.	-0.550	0.339	0.200	2.341
10.	0.115	0.253	0.309	3.344
11.	0.267	0.136	0.308	3.555
12.	0.291	-0.058	0.263	3.545

Table 12. Model VI- inverse wind, $x=0.8$

$\log M_{lum}(M_{\odot})$	$\langle [Fe/H] \rangle_*$ (dex)	$\langle [Mg/Fe] \rangle_*$ (dex)	Mg_2 (mag)	$\langle Fe \rangle$ (\AA)
9.	-0.099	0.340	0.287	3.040
10.	-0.091	0.365	0.294	3.064
11.	-0.023	0.368	0.308	3.168
12.	-0.005	0.390	0.316	3.188

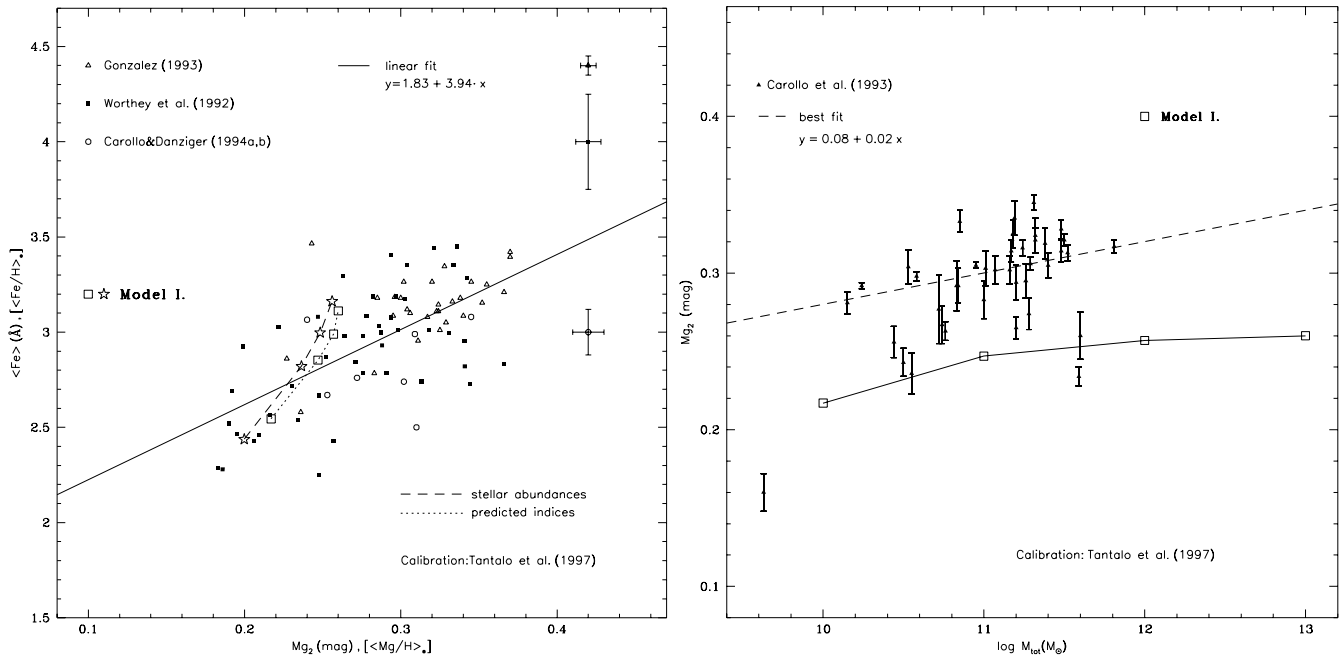


Fig. 1. a (left panel) Predicted and observed metallicity indices. The dotted line and open squares represent the $\langle Fe \rangle$ versus Mg_2 predicted by Model I for galaxies of different masses, as indicated in Table 7. The dashed line and stars represent the real abundances of Fe and Mg as predicted by Model I for galaxies of different masses and arbitrarily translated in the $\langle Fe \rangle$ vs. Mg_2 diagram. The error bars referring to the different data samples are also shown. **b** (right panel) Predicted and observed Mg_2 versus mass relation. The predictions are from Model I.

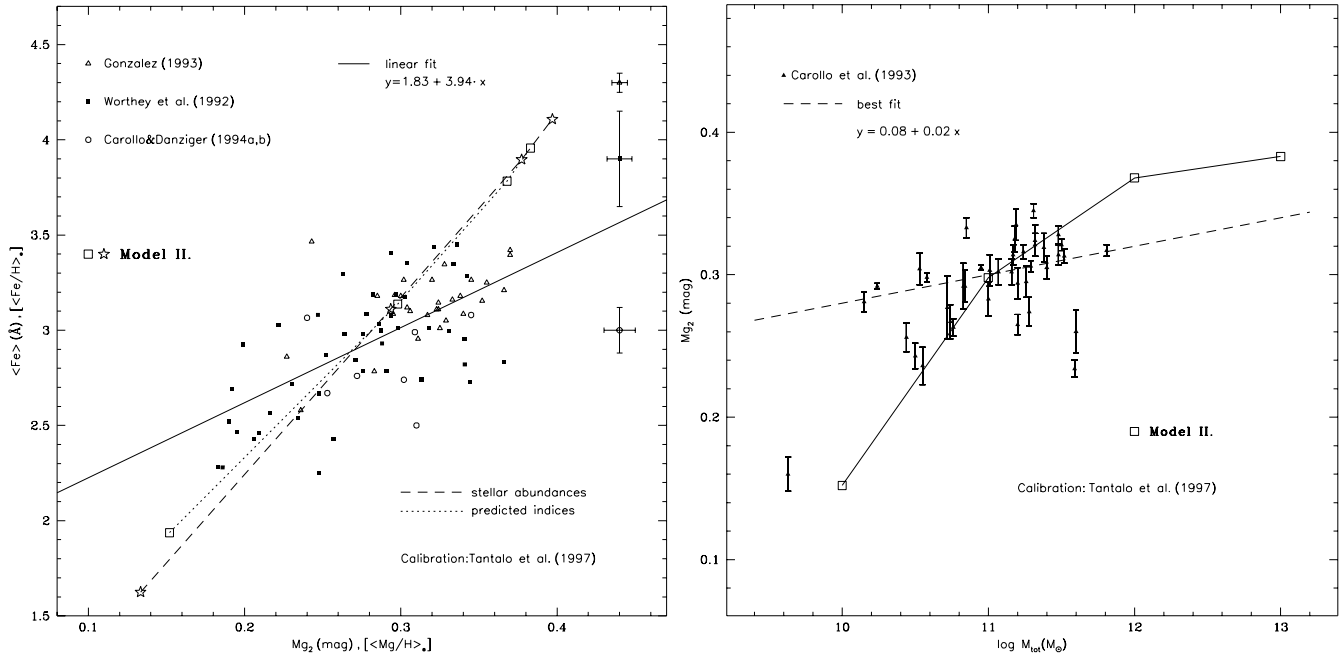


Fig. 2. **a** The same as Fig. 1a but relative to the predictions of Model II. **b** The same as Fig. 1b but relative to the predictions of Model II.

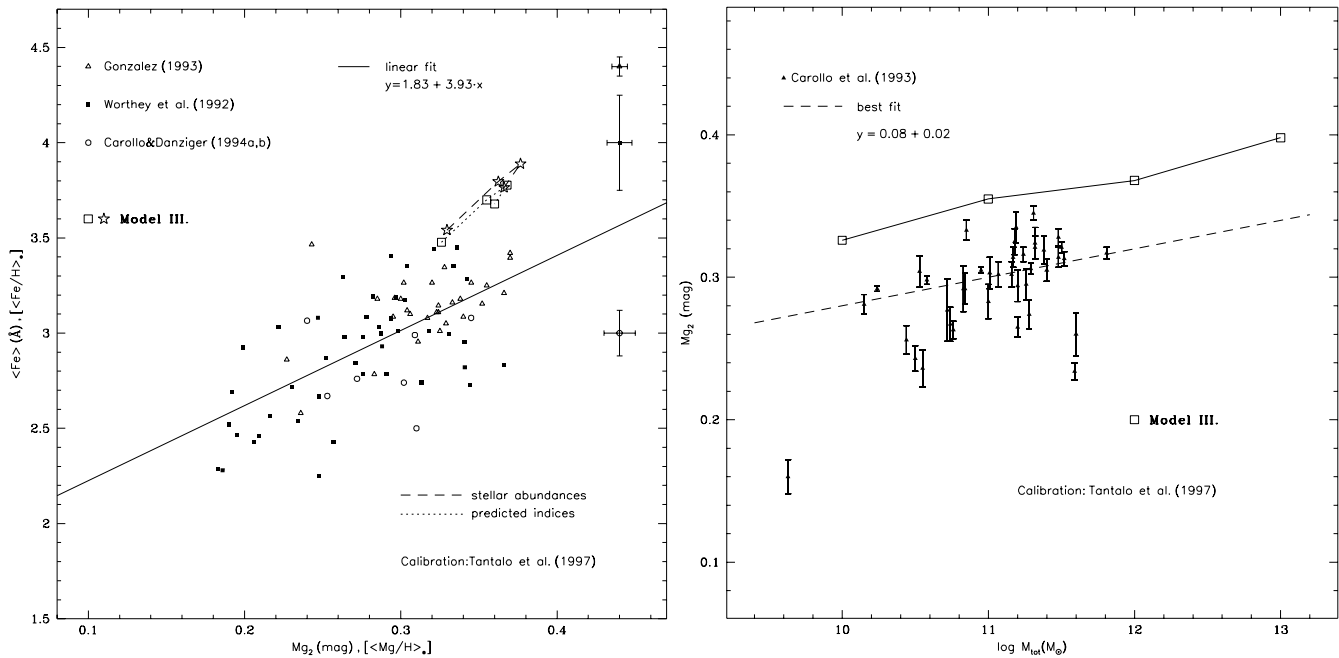


Fig. 3. **a** The same as Fig. 1a but for the predictions of Model III. **b** The same as Fig. 1b but for the predictions of Model III.

One criticism that could in principle be moved to the results discussed before is that we adopted mass-averaged metallicities and not luminosity-averaged metallicities, as it should be the case. In Fig. 9 we show the indices obtained by the luminosity- and mass-averaged metallicities calculated for the results of Model II, when the calibration of Tantaló et al. (1998) is applied. The luminosity-averaged metallicities, computed with the photometric model of Gibson (1997), are systematically slightly lower than the others and the difference is larger for smaller

galaxies, as expected. However, the slope is the same in the two cases, showing that the use of mass-averaged metallicity for this kind of analysis is quite justified.

5. Discussion and conclusions

In this paper we have discussed the relation between metallicity indices, such as Mg_2 and $\langle Fe \rangle$, and total mass in nuclei of ellipticals and its implications in terms of models of formation and evolution of elliptical galaxies.

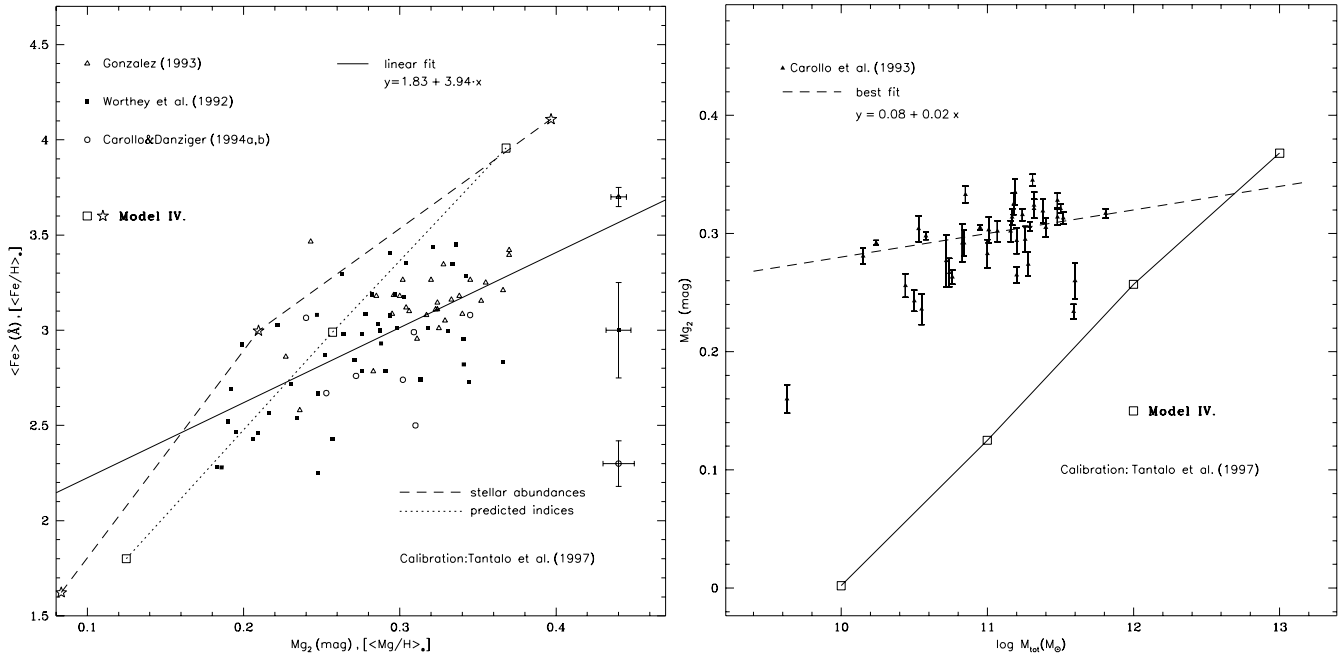


Fig. 4. **a** The same as Fig. 1a but for the predictions of Model IV. **b** The same as Fig. 1b but for the predictions of Model IV.

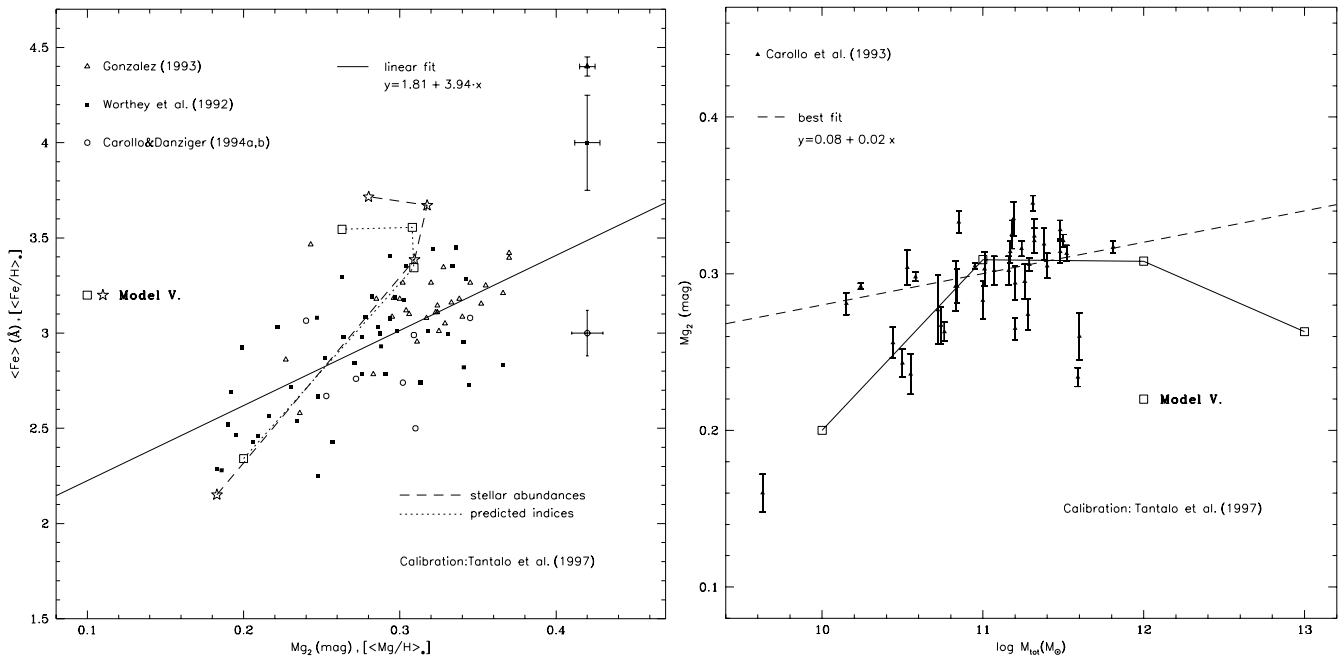


Fig. 5. **a** The same as Fig. 1a but for the predictions of Model V. **b** The same as Fig. 1b but for the predictions of Model V.

In order to do that we have transformed the average abundance of Fe in the composite stellar population of the galaxy, as predicted by different models of chemical evolution, into Mg_2 and $\langle Fe \rangle$ indices by means of the available calibrations.

We have shown the results of classic wind models for ellipticals, such as those discussed by Arimoto and Yoshii (1987) and Matteucci and Tornambè (1987), as well as the results of models with variable IMF from galaxy to galaxy and with galactic winds occurring first in the more massive systems, implying

that these systems are older than the less massive ones. We have found that it is not possible to establish clearly which kind of model should be preferred, first of all because of the large spread present in the data.

Moreover, little difference is found in the predicted indices of models which predict a $[\langle Mg/Fe \rangle]_*$ either increasing or decreasing with galactic mass, although the data seem to suggest an increase of this ratio with galactic mass larger than predicted by any of the models.

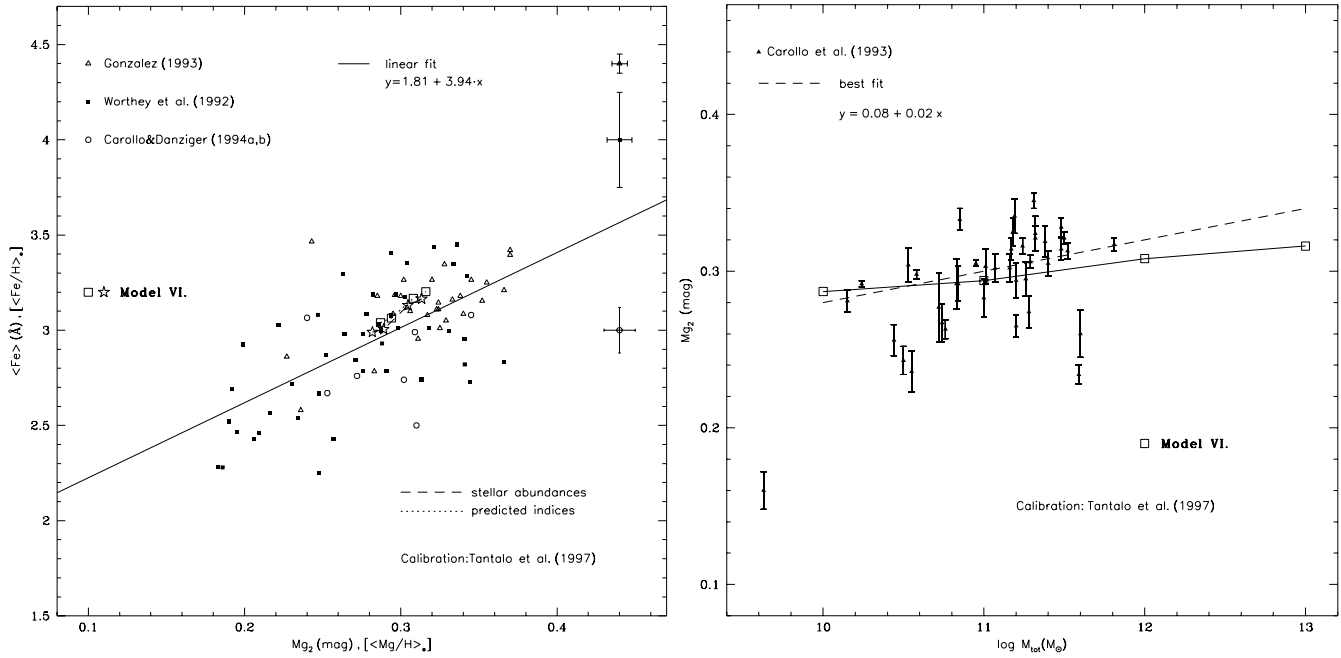


Fig. 6. **a** The same as Fig. 1a but for the predictions of Model VI. **b** The same as Fig. 1b but for the predictions of Model VI.

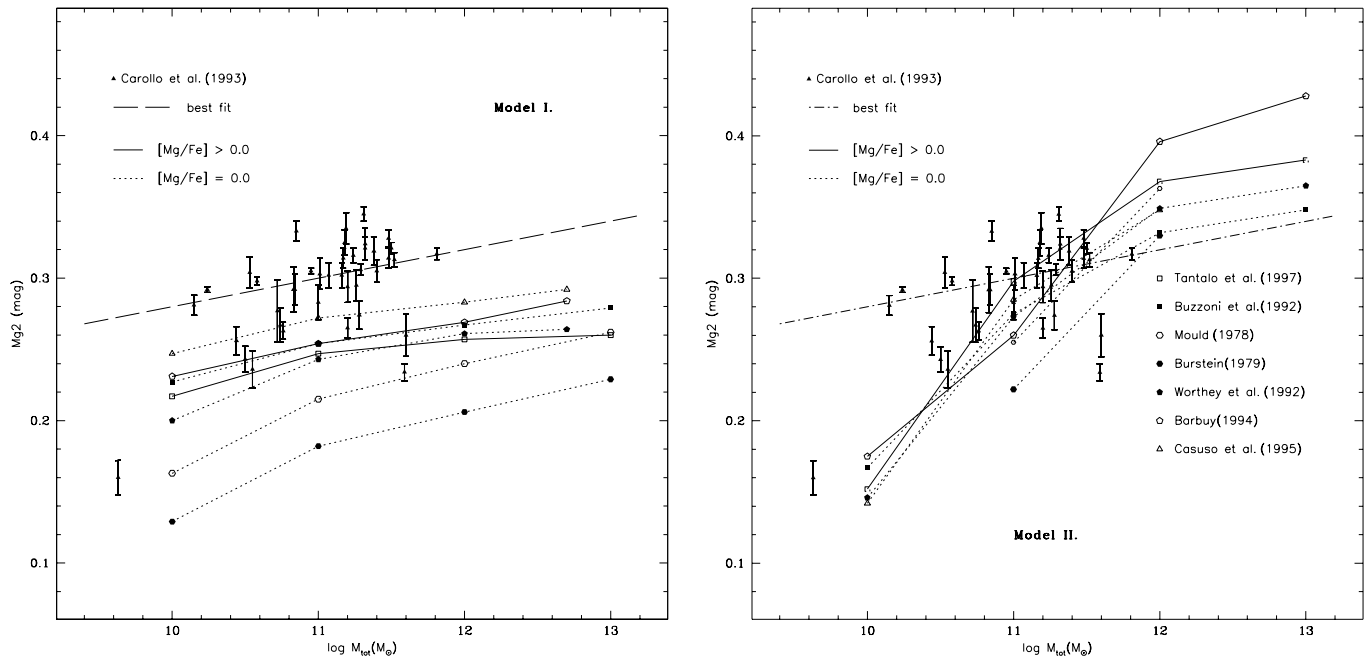


Fig. 7. Mg_2 -mass relationships as predicted by Model I by using different calibrations, as indicated in Fig. 8. The best-fit to the data is also shown.

Fig. 8. Mg_2 -mass relationships as predicted by Model II by using different calibrations, as indicated in the figure. The best-fit to the data is also shown.

On this basis, the classic wind model can not be considered worse than the other models. Actually, the classic wind model with a flat constant IMF seems to be the only one which can reproduce the whole range of the observed indices. However, if we isolate the data from Gonzalez (1993) and do not consider the others, then in order to reproduce the flat slope of the $\langle Fe \rangle$ versus Mg_2 relation, as given by the best-fit of the data,

one should assume that Fe among the nuclei of ellipticals is almost constant whereas Mg increases from less massive to more massive nuclei. This is not achieved by any of the models presented here since it would require quite “ad hoc” assumptions especially concerning the type Ia SNe.

From the numerical experiments performed in this paper we can say that a model which explains at the same time the

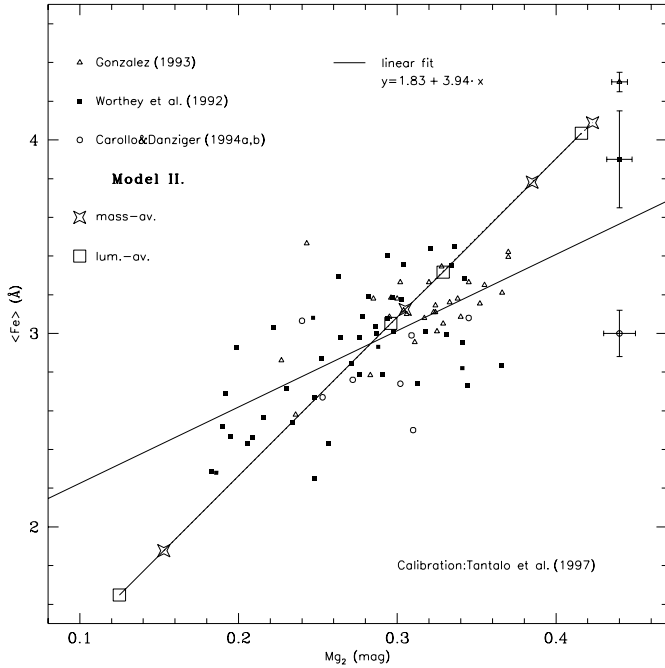


Fig. 9. Predicted and observed $\langle Fe \rangle$ versus Mg_2 . The predicted indices, relative to Model II, are calculated by averaging on the mass (stars) and on the visual luminosities (squares).

mass-metallicity and the iron-magnesium relation requires an inverse wind situation, with a strong increase of the star formation efficiency with galactic mass (i.e. Model VI), rather than a variable IMF from galaxy to galaxy, and an IMF with a slope $x = 0.8$. However, a model of this type is not able to reproduce the observed ranges of $\langle Fe \rangle$ and Mg_2 . We have also calculated models where amount and concentration of dark matter increases, compatibly with the formulation of the potential energy of the gas, with decreasing galactic luminous mass (see Persic et al. 1996), with the net result of obtaining an “inverse wind” situation. The results are very similar to those of Model III. Therefore, to obtain a better agreement with observations one should invoke also in this case an increase of the star formation efficiency with galactic mass. This would certainly flatten the $\langle Fe \rangle$ vs. Mg_2 relation but it would further shrink the ranges of the predicted indices. In fact, both an increasing star formation efficiency and a decreasing importance of dark matter with increasing luminous galactic mass can be viable solutions to achieve the situation of more massive ellipticals being older than less massive ones.

In conclusion, it is quite important to establish the value of [Mg/Fe] from the observational point of view since abundance ratios, such as [Mg/Fe], represent an important diagnostic to infer ages in galaxies, due to the different timescales for the Mg and Fe production. Generally, a high [Mg/Fe] is interpreted as a young age and the upper limit for the age is given by the time at which the chemical enrichment from type Ia SNe starts to become important. This timescale depends not only on the assumed progenitors of type Ia SNe but also on the star formation history of the galaxy considered (see Matteucci 1997)

and for giant elliptical galaxies this timescale is of the order of $t_{SNeIa} \sim 3 - 4 \cdot 10^8$ years and in any case it can not be larger than 1 Gyr also for smaller systems. This is at variance with what stated by Kodama and Arimoto (1997) who claim, on the basis of results concerning our Galaxy (Yoshii et al. 1996), that this timescale is of the order of 1.5-2.5 Gyr. This is indeed true for our Galaxy where the star formation history has been quite different than in ellipticals and it had been already pointed out in Greggio and Renzini (1983) and in Matteucci and Greggio (1986). This is a quite important point, both for the galactic chemical enrichment and for the predictions about SN rates at high redshift.

Therefore, an enhanced [Mg/Fe] indicates that the process of galaxy formation must have been very fast thus favoring a monolithic collapse scenario rather than a merging scenario. In this framework, a [Mg/Fe] ratio higher in more massive ellipticals than in less massive ones could be interpreted as due to their faster formation and evolution (see Matteucci 1994; Bressan et al. 1996).

An independent way of estimating the ages of ellipticals, where for ages we intend the time elapsed from the last star formation event, is to study the H_β index. This index is, in fact, related to the age of the dominant stellar population, since it gives a measure of the turn-off color and metallicity. It can therefore be used to solve the age-metallicity degeneracy. Bressan et al. (1996), by analyzing the H_β and other physical parameters in the sample of ellipticals observed by Gonzalez (1993), concluded that massive galaxies should have stopped forming stars before less massive ones, in agreement with the results of the inverse wind model discussed here. Finally, we would like to point out that both models with a Salpeter IMF and a variable IMF have a potential problem in reproducing high $[\alpha/Fe]$ ratios in the intracluster medium (ICM), as shown by their low average $[\langle \alpha/Fe \rangle]$ ratios (see Tables 7-12). Therefore, in agreement with MG95 and Gibson and Matteucci (1997) we conclude that a flat IMF is required to explain the high $[\alpha/Fe]$ ratios, as found by ASCA observations (Mushotzky 1994).

Acknowledgements. One of us (F.M.) wants to thank F. Carbognani for his help with the data fitting procedures. We also like to thank the referee G. Worthey for his careful reading and his suggestions.

References

- Arimoto, N., Yoshii, Y. 1987, A&A 173, 23
- Barbuy, B. 1994 Ap.J. 430, 218
- Bender, R., Burstein, D. & Faber, S.M.: 1992, Ap.J. 399,462
- Bender, R., Ziegler, B., Bruzual, G. 1996, Ap.J. 463, L51
- Borges, A.C., Idiart, T.P., de Freitas-Pacheco, J.A., Thevenin, F. 1995 A.J. 110, 2408
- Bressan, A., Chiosi, C., Fagotto, F. 1994 Ap.J. Suppl. 94, 63
- Bressan, A., Chiosi, C. Tantalò, R. 1996 A&A 311, 425
- Brocato, E., Matteucci, F., Mazzitelli, I. & Tornambè, A.: 1990, Ap.J. 349, 458
- Bruzual, G., Charlot, S. 1993 Ap. J. 405, 538
- Burstein, D. 1979 Ap. J. 232, 74
- Buzzoni, A. Gariboldi, G., Mantegazza, L. 1992 A.J. 103, 1814
- Carollo, C.M., Danziger, I.J., Buson, L.: 1993, MNRAS 265, 553

- Carollo, C.M., Danziger, I.J. 1994a, MNRAS 270, 523
Carollo, C.M., Danziger I.J. 1994b, MNRAS 270, 743
Casuso, E., Vazdekis, A., Peletier, R., Beckman, J.E. 1996 Ap.J. 458, 533
Charlot, S., Worthey, G., Bressan, A. 1996 Ap. J. 457, 625
Chiosi, C., Bressan, A., Portinari, L., Tantalo, R. 1998, A&A in press
Cox, D.P. 1972 Ap.J. 178, 159
Davies, R.L., Sadler, E.M. & Peletier, R.: 1993, MNRAS 262, 650
Faber, S.M., Worthey, G. & Gonzalez J.J. 1992, in *IAU Symp. n.149*, eds. B. Barbuy and A. Renzini, p. 255
Faber, S.M., Burstein, D., Dressler, A. 1977, A.J. 82, 941
Faber, S.M., Freiel, E.D., Burstein, D., Gaskell, C.M. 1985, Ap.J. Suppl. 57, 711
Gibson, B., K. 1994 MNRAS 271, L35
Gibson, B.K. 1997, MNRAS 290, 471
Gibson, B.K., Matteucci, F., 1997. MNRAS, 291, L8
Gonzalez, J.J. 1993 PhD Thesis, University of California, Santa Cruz
Greggio, L., 1996, MNRAS 285, 151
Greggio, L., Renzini, A. 1983, in *"The First Stellar Generations"*, Mem. Soc. Astron. It., Vol. 54, p.311
Kodama, T., Arimoto, N. 1997, A&A 320, 41
Larson, R.B. 1974 MNRAS 169, 229
Matteucci, F. 1992 Ap.J. 397, 32
Matteucci, F. 1994 A&A 288, 57
Matteucci, F. Gibson, B.K. 1995 A&A 304, 11 (MG95)
Matteucci, F., Greggio, L.: 1986, A&A 154, 279
Mould, J.R. 1978 Ap.J. 220, 434
Mushotzsky, R. 1994 in "Clusters of Galaxies" ed. F. Durret et al. Editions Frontieres p.167
Nomoto, K., Thielemann, F. K. & Yokoi, K.: 1984, Ap.J. 286, 644
Padoan, P., Nordlund, A.P., Jones, B.J.T. 1997, MNRAS 288, 145
Padovani, P., Matteucci, F. 1993 Ap.J. 416, 26
Peletier, R., 1989, PhD Thesis, University of Groningen
Persic, M., Salucci, P., Stel, F. 1996 MNRAS 281, 27
Renzini, A., Voli, M.: 1981, A&A 94, 175
Salpeter, E. E.: 1955, Ap.J. 121, 161
Tantalo, R., Chiosi, C., Bressan, A. 1998 A&A 333, 419
Thielemann, F.K., Nomoto, K., Hashimoto, M. 1993 *Origin and Evolution of the Elements*, ed. N. Prantzos et al., Cambridge Univ. Press p. 297
Tinsley, B.M., Larson, R.B. 1979 MNRAS 186, 503
Weiss, A., Peletier, R., & Matteucci, F.: 1995 A&A 296, 73
Worthey, G. 1994 Ap.J. Suppl. 95, 107
Worthey, G., Faber, S.M. & Gonzalez, J.J.: 1992, Ap.J. 398, 73
Woosley, S.E., Weaver, T.A. 1986 Ann. Rev. Astron. Astrophys. 24, 205
Woosley, S. E.: 1987, in *"Nucleosynthesis and Chemical Evolution"*, 16th Saas Fee Course, eds. B. Hauck et al. (Geneva: Geneva Observatory), p.1
Yoshii, Y., Arimoto, N. 1987 A&A 188, 13
Yoshii, Y., Tsujimoto, T., Nomoto, K. 1996, Ap.J. 462, 266